Starch ester film properties

Boetje, Laura; Lan, Xiaohong; van Dijken, Jur; Woortman, Albert J.J.; Popken, Thijs; Polhuis, Michael; Loos, Katja

Published in:
Carbohydrate Polymers

DOI:
10.1016/j.carbpol.2023.121043

Publication date:
2023

Carbohydrate Polymers 316 (2023) 121043

Contents lists available at ScienceDirect

Carbohydrate Polymers

journal homepage: www.elsevier.com/locate/carbpol

Starch ester film properties: The role of the casting temperature and starch its molecular weight and amylose content

Laura Boetje [a], Xiaohong Lan [a], Jur van Dijken [a], Albert J.J. Woortman [a], Thijs Popken [a], Michael Polhuis [b], Katja Loos [a,*]

[a] Macromolecular Chemistry & New Polymeric Materials, Zernike Institute for Advanced Materials, University of Groningen, Nijenbogh 4, 9747AG Groningen, the Netherlands

[b] Royal Avebe U.A., Zernikelaan 8, 9747AA Groningen, the Netherlands

ARTICLE INFO

Keywords:
Fatty acid starch ester
Antibacterial
Thermoplastic
Starch film
Mechanical properties

ABSTRACT

Oleic acid and 10-undecenoic acid were used to esterify corn, tapioca, potato and a waxy potato starch, with a maximum degree of substitution of 2.4 and 1.9 respectively. The thermal and mechanical properties were investigated as a function of the amylopectin content and M_w of starch, and by the fatty acid type. All starch esters had an improved degradation temperature regardless of their botanical origin. While the T_g did increase with increasing amylopectin content and M_w, it decreased with increasing fatty acid chain length. Moreover, films with different optical appearances were obtained by varying the casting temperature. SEM and polarized light microscopy showed that films cast at 20 °C had porous open structures with internal stress, which was absent when cast at higher temperatures. Tensile test measurements revealed that films had a higher Young's modulus when containing starch with a higher M_w and amylopectin content. Besides that, starch oleate films were more ductile than starch 10-undecenoate films. In addition, all films were resistant to water at least up to one month, while some light-induced crosslinking took place. Finally, starch oleate films showed antibacterial properties against *Escherichia coli*, whereas native starch and starch 10-undecenoate did not.

1. Introduction

Starch comprises two major components, amylose and amylopectin, both consisting of glucose molecules (Ahmadi-Abhari, Woortman, Hamer, & Loos, 2015; Van Soest, Hulleman, De Wit, & Vliegenthart, 1996). Amylose is an essentially linear molecule in which an α(1 → 4) glycosidic bond links the glucose molecules together, while amylopectin is branched with α(1 → 6) glycosidic bonds as its branch points (Buléon, Colonna, Planchot, & Ball, 1998; French, 1972). The M_w of amylopectin ($\sim 10^8$ Da) is approximately 100 times higher than that of amylose (Costas, 1998; Mua & Jackson, 1997; Van Soest & Vliegenthart, 1997). Starch can be found in potatoes, corn, rice, tapioca, etc., and its botanical origin influences the ratio of amylose and amylopectin, as well as its weight average molecular weight (M_w), which in turn affects the film's mechanical properties (Fredriksson, Silverio, Andersson, Eliasson, & Åman, 1998).

Starch is abundant in nature and low in cost, which are both good characteristics when acting as a replacement for the current petroleum-based plastic films. Unfortunately, native starch suffers from some drawbacks like its poor solubility in organic solvents, brittleness of films, and susceptibility to water absorption (Fang, Fowler, Tomkinson, & Hill, 2002; Henning Winkler, Vorwerg, & Wetzel, 2013). Moreover, native starch has without any plasticizer no visible glass transition temperature (T_g), which makes processing nearly impossible (Ciardelli & Penczek, 2004; Niranjana Prabhu & Prashantha, 2018; Zhang, Rempel, & Liu, 2014). The aforementioned drawbacks limit its direct use, but a common strategy to overcome those is via the substitution of hydroxyl groups with fatty acids (Niranjana Prabhu & Prashantha, 2018). Each anhydroglucose unit (AGU) contains three hydroxyl groups, enabling a maximum degree of substitution (DS) of 3 (Konieczny & Loos, 2018). The addition of fatty acids breaks the intra- and intermolecular hydrogen bonds in the polymer chains, opening up the starch network. This process increases the free volume of starch, thereby lowering the T_g (Van Soest & Vliegenthart, 1997).

In addition to imparting thermoplastic properties to starch, fatty acids are known to have antibacterial properties against, for example,

* Corresponding author.
E-mail addresses: l.boetje@rug.nl (L. Boetje), x.lan@rug.nl (X. Lan), j.van.dijken@rug.nl (J. van Dijken), a.j.j.woortman@rug.nl (A.J.J. Woortman), t.popken1@student.rug.nl (T. Popken), michael.polhuis@avebe.com (M. Polhuis), k.u.loos@rug.nl (K. Loos).

https://doi.org/10.1016/j.carbpol.2023.121043
Received 20 December 2022; Received in revised form 16 May 2023; Accepted 19 May 2023
Available online 25 May 2023

Escherichia coli (*E. coli*) and *Staphylococcus aureus* (*S. aureus*), both of which are common in the spoilage of food (Harris, 1997; Yunbin Zhang, Liu, Wang, Jiang, & Quek, 2016). Packaging material with antibacterial properties prevents food spoilage and increases food safety, making modified starches appealing for such applications as well (Huang, Qian, Wei, & Zhou, 2019; Malhotra, Keshwani, & Kharkwal, 2015; Motelica et al., 2020; Sung et al., 2013; Tharanathan, 2003).

Recent research shows the effect of the fatty acid chain length and DS on the thermal and mechanical properties of starch films; however, the effect of starch botanical origin on highly substituted starches is hardly documented (Vanmarcke et al., 2017; Zhu et al., 2017). Additionally, most research to date focuses on the antibacterial properties of free fatty acids, while only some on methyl esters, and sugar esters (Chandrasekaran, Senthilkumar, & Venkatesalu, 2011; Dilika, Bremner, & Meyer, 2000). Studies on sugar esters usually involve simple sugars such as sucrose, lactose, or fructose (Perinelli et al., 2018; Zhao, Zhang, Hao, & Li, 2015), while limited research exists into esters of carbohydrates such as starch.

We studied the influence of the botanical origin on the thermal and mechanical properties of synthesized starch esters. Potato starch was compared with waxy potato starch, as well as two starches from different botanical sources with varying amylopectin contents and molecular weights (corn and tapioca starch). By varying the botanical origin, we obtain information about both the influence of the M_w and the amylopectin content. We performed an esterification with two different unsaturated fatty acids, 10-undecenoic acid and oleic acid, to assess the fatty acid's influence on the resulting properties and its antibacterial effect. These widely available fatty acids have an unsaturated bond, which could be interesting for further modification of the resulting materials, for example by crosslinking or addition of thiol-containing molecules. The effect of the casting temperature on the mechanical properties of starch films was tested. We strive to make an antibacterial biobased material with improved mechanical and thermal properties that could be used to replace conventional plastic.

2. Experimental

2.1. Materials

Avebe kindly provided potato starch (Paselli WA4, PS) and waxy potato starch (Eliane C100, WPS). Corn starch (CS) and tapioca starch (TS) were purchased from Sigma Aldrich and Holland and Barret, respectively. Before use, all starches were dried overnight at 110 °C and stored in a desiccator over silica gel and P_2O_5. Oleic acid (90 %), 1,1-carbonyldiimidazole (CDI, ≥97 %), chloroform-d_6 ($CDCl_3$, 99.8 %), and methanol-d_4 (MeOD, 99 %) were purchased from Sigma–Aldrich. Dimethyl sulfoxide (DMSO, ≥99.7%) was purchased from J.T. Baker, and 10-undecenoic acid (>95.0 %) from TCI Europe. Macron Fine Chemicals supplied methanol (MeOH, ≥99.8 %) and chloroform ($CHCl_3$) while, Biosolve supplied tetrahydrofuran (THF, 99.85 %). All chemicals were used without further purification unless stated otherwise.

2.2. Starch esters

2.2.1. Esterification of starch

Steglich esterification offers mild reaction conditions while still being effective (Heinze, Libert, & Koschella, 2006). The most common activating agent is 1,3-dicyclohexylcarbodiimide (DCC) with 4-dimethylaminopyridine as the catalyst. Although the reaction conditions are mild, both chemicals are toxic (Tremblay-Parrado, García-Astrain & Avérous, 2021). N,N′-carbonyldiimidazole (CDI) is a mild and efficient alternative for DCC, as this activating agent is less toxic and no undesired side products are formed (Hussain, Liebert, Heinze, & Jena, 2004). Moreover, it allows the use of dimethyl sulfoxide (DMSO) as a solvent in contrast to DCC, which requires DMAc/Li (Heinze et al., 2006). This is why CDI is preferred over DCC.

The method is based on literature and shown in Scheme 1 (Blohm & Heinze, 2019). In a round bottom flask, 4 g of starch was dissolved in 120 mL DMSO by heating it in an 80 °C oil bath. Oleic acid or 10-undecenoic acid (1.6 eq. per –OH of starch) was dissolved in a second round bottom flask in 40 mL of DMSO and heated to 60 °C. The activating agent, CDI (1.6 eq. per -OH) was added to the fatty acid solution and stirred for 30 min to activate the fatty acids. The activated fatty acid solution was added to the starch solution and stirred for 16 h at 80 °C, resulting in the formation of a gel. The gel was precipitated in MeOH, dissolved in $CHCl_3$ and precipitated again (3×). A white solid was obtained and dried in a vacuum oven at 40 °C overnight.

2.2.2. Starch ester characterization

2.2.2.1. Static light scattering. Prior to measurement, all unmodified starches were pregelatinized in water, after which they were freeze-dried. The starches were dissolved in DMSO with LiBr (0.05 M) by heating at 100 °C for 1 h followed by stirring at room temperature for 1 day. For each different type of starch, 5 different concentrations were made ranging between $6\bullet10^{-5}$ g•mL^{-1} and $3\bullet10^{-4}$ g•mL^{-1}. The measurements were performed on a MALLS detector (632.8 nm), Dawn DSP with F2 batch cell, Wyatt Technology calibrated with toluene. The samples were filtered over a 5.0 μm filter, and the measurement was performed using 11 different angles, with dn/dc = 0.072 and RI = 1.478. For each sample, the measurements were performed at least in duplicate. The weight average molecular weight (M_w) and the radius of gyration (R_g) were determined from the Berry plot and established from Eq. (1).

$$\left(\frac{KC}{R_\theta}\right)^{0.5} = \left(\frac{1}{M_w}\right)^{0.5}\left(1+\frac{q^2R_g^2}{M_w}\right)(1+A_2M_wC) \quad (1)$$

In Eq. (1), K represents the optical constant, and C is the concentration of the starch solution in g•mL^{-1}. R_θ is the Rayleigh ratio at angle θ in nm^{-1}, M_w is the weight-average molecular weight in g•mol^{-1}, R_g is the radius of gyration in nm and q is the scattering vector in nm, which is based on the refractive index of the solvent and the wavelength of the laser used, and finally, A_2 is the second virial coefficient in mL•mol•g^{-2}.

2.2.2.2. ^1H NMR spectroscopy. The ^{1}H NMR spectra were recorded on a Varian 400 MHz NMR spectrometer. The DS was calculated according to Eq. 2 (Boetje et al., 2022). In Eq. (2), N represents the protons present in the double bond, which is 2 and 3 for SO and S10U, respectively. The protons in the range 4.7–6 ppm were integrated and their total value was represented by X. For SO, the integration was normalized to oleic acid's terminal methyl group with a value of 3. For S10U, the spectra were normalized to the peak at 1.9 ppm corresponding to 2 protons.

$$\frac{3DS}{N^*DS+(3-DS)} = \frac{3}{X} \quad (2)$$

The ^{1}H NMR and ATR-FTIR specifications of the starch esters from different botanical sources are similar; therefore, only starch 10-undecenoate (S10U) and starch oleate (SO) from potato starch are presented below. Spectra for the remaining starch esters that were synthesized can be found in the supplementary information.

^1H NMR spectra

S10U from potato starch

^{1}H NMR (400 MHz, $CDCl_3$, δ, ppm): 5.76 (1H, br, =CH-CH_2), 5.41 (1H, br, -C3-OH), 5.27 (H, br, -C2-OH), 4.90 (2H, q, =CH_2), 4.78 (1H, br, -C1H-), 4.63 (1H, br, -C6H_2-OH), 4.12 (2H, br, -C6H_2-), 3.90 (1H, br, -C3H-), 3.84 (1H, br, -C5H-), 3.68 (1H, br, -C2H-), 3.56 (1H, br, -C4H-), 2.28 (2H, br, -CO-CH_2-), 1.94 (2H, q, -CH_2-C=), 1.53 (2H, br, -CO-CH_2-CH_2-), 1.20 (10H, br, -CH_2-CH_2-CH_2-CH_2-CH_2-CH_2-C=).

SO from potato starch

^{1}H NMR (400 MHz, $CDCl_3$, δ, ppm): 5.39 (1H, br, -C3-OH), 5.31 (2H,

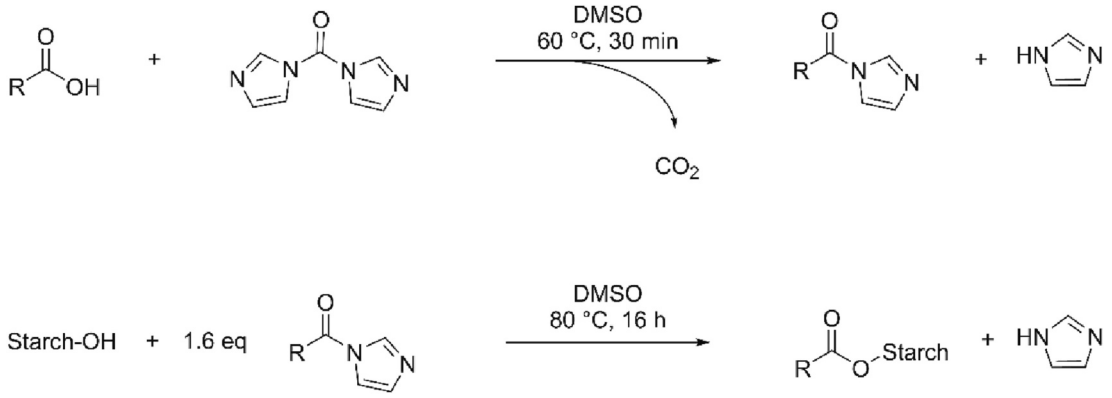

Scheme 1. Synthesis of starch esters via activation of CDI in two steps.

br, -CH=CH-), 5.27 (1H, br, -C2H-OH), 4.75 (1H, br, -C1H-), 4.43 (1H, br, -C6H_2-OH), 4.08 (2H, br, -C6H_2-), 3.97 (1H, br, -C3H-), 3.87 (1H, br, -C5H-), 3.68 (1H, br, -C2H-), 3.56 (1H, br, -C4H-), 2.33 (2H, br, -O-CH_2-), 1.99 (4H, br, -CH_2-CH=CH-CH_2-), 1.58 (6H, br, -O-CH_2-CH_2-, -CH_2-CH_2-CH=CH-CH_2-CH_2-), 1.25 (14H, br, -CO-CH_2-CH_2-CH_2-CH_2-CH_2-, -CH_2-CH_2-CH_2-CH_2-CH_2-CH_3) 0.86 (3H, t, -CH_3-).

2.2.2.3. Fourier transform infrared spectroscopy (FT-IR). Measurements were conducted on a vertex 70 Bruker spectrometer in attenuated total reflectance (ATR) mode. The resolution was 16 cm^{-1}, with both a sample and background scan time of 32 scans. The data were analyzed with OPUS software, in which a background correction was performed and the data were normalized using the band at 1030 cm^{-1}.

ATR-FTIR spectra

S10U from potato starch

ATR-FTIR (ν, cm^{-1}): 3280 (-OH stretching of unsubstituted hydroxyl groups of starch); 3031 (C=C stretching of 10-undecenoate); 2928 (C—H stretching of 10-undecenoate); 1740 (C=O stretching of 10-undecenoate); 1653 (C=C stretching of 10-undecenoate); 1464 (C—H bending, of the alkyl -CH_3 of oleate); 1378 (C—H bending, of the alkyl -CH_3 of oleate); 1149 (C—O stretching, from the formed ester); 1023 (O—C stretching of anhydroglucose ring of starch).

SO from potato starch

ATR-FTIR (ν, cm^{-1}): 3280 (-OH stretching of unsubstituted hydroxyl groups of starch); 3008 (ν, stretching, C=C stretch of oleate), 2928 (C—H stretching of oleate); 1740 (C=O stretching of oleate); 1464 (C—H bending, of the alkyl -CH_3 of oleate); 1378 (CH-bending, of the alkyl -CH_3 of oleate); 1149 (C—O stretch, from the formed ester), 1023 (O—C stretching of anhydroglucose ring of starch).

2.2.2.4. Thermogravimetric analysis (TGA). Thermal stabilities were determined by thermal gravimetric analysis (TGA). The degradation temperature was established on a TA-instrumental 5500. The sample was heated under an inert atmosphere (N_2) from 25 to 700 °C at a rate of 10 °C•min^{-1}. The data were analyzed by TRIOS software (TA instruments) and used to determine the degradation temperature where the rate of weight loss is maximum.

2.2.2.5. Differential scanning calorimetry (DSC). Glass transition temperatures were determined by DSC measurements performed on a TA-Instruments Q1000. The sample (5–10 mg) was weighed in a non-hermetically closed aluminum pan against an empty reference dish. A heat-cool-heat cycle from −20 °C to 200 °C was performed under nitrogen at a rate of 10 °C•min^{-1}. The first heating cycle removed residual solvent traces from the starch ester; therefore, only the second heating cycle is presented.

2.3. Starch ester films

2.3.1. Film casting

Films were cast by dissolving 1.5 g of starch ester in 50 mL chloroform or THF. The solution was degassed by sonication in a water bath at room temperature for 30 min to remove air from the solvent. Following sonication, the solution was poured into a square Teflon dish with a surface area of 100 cm^2 and allowed to evaporate at a temperature of 20, 40, 60, or 80 °C.

2.3.2. Characterization of the films

2.3.2.1. Light microscopy. Films were analyzed on a Nikon light microscope (Nikon, Eclipse 600, Japan) under polarized light with a lambda filter. The images were captured with a Nikon camera with a 40× magnification lens (Nikon, COOLPIX 4500, MDC Lens, Japan).

2.3.2.2. Scanning electron microscopy. Before analysis, the samples were sputtered with gold. The images were recorded on a Philips XL30 field emission gun scanning electron microscope with EDAX EDS/EBSD detectors. The images were obtained with a 5 kV accelerated voltage and 1000× magnification.

2.3.2.3. X-ray diffraction (XRD). The structures were analyzed on a Bruker D8 Advanced apparatus. The sample was measured between 4 and 50° at the 2θ angle at 40 kV and 40 mA using Cu Kα radiation (λ = 0.1542 nm).

2.3.2.4. Tensile test. Dog-bone-shaped halters were cut from the cast films. The tensile test was performed on an Instron 5565 machine with a 100 N load cell and a pulling speed of 2 mm s^{-1}. The average of five samples was taken, including the standard deviation.

2.3.2.5. Antibacterial test. Starch ester films were tested for antibacterial resistance against *Escherichia coli* (*E. coli*, 0157 K) and *Staphylococcus aureus* (*S. aureus*, ATCC12600), with a 3 M™ Petrifilm™ Aerobic Count Plate test purchased from 3 M Science Applied to Life™. The test was done as described in literature before (Keskin et al., 2020). The bacterial solutions were prepared as follows: The bacteria were incubated in 10 mL tris-buffered saline (TBS) solution at 37 °C for 24 h, after which they were further grown for 16 h in 200 mL TBS at 37 °C. The solution was subsequently centrifuged three times at 6500 rpm, washed with phosphate-buffered saline solution (PBS), sonicated for 30 s, and diluted 100-fold. The number of bacteria present was counted. The solution was further suspended to a concentration of 10^2 bacteria•mL^{-1}. Films from native potato starch, S10U and SO were tested. The films had dimensions of 2 cm by 2 cm and were sterilized under UV light (254 nm) for 1 h. Once sterilized, the films were placed on agar that was already

present at the 3 M™ Petrifilm™ Aerobic Count Plate test. On each film, a 20 μL bacteria solution was pipetted. The films were incubated for 48 h at 37 °C. After incubation, the number of bacteria was established by counting the visible red spots. The fatty acid double bond might be affected during sterilization by UV irradiation, and its presence after irradiation was determined by ^{1}H-HNMR spectroscopy and was found to be 89 % for SO and 100 % for S10U.

3. Results and discussion

3.1. Starch ester analysis

3.1.1. Static light scattering

The M_w and amylose content of starch differ depending on the botanical origin (Fredriksson et al., 1998). Therefore, different starches were studied with static light scattering to obtain their M_w, and radius of gyration (R_g). The R_g is dependent on the M_w of the starch but is also related to the amount of amylose and amylopectin present. Linear chains, such as amylose, have a higher R_g than branched structures like amylopectin (Millard, Dintzis, Willett, & Klavons, 1997), therefore the R_g can provide information on the amylose content. Table 1 states the static light scattering results, which shows that corn starch (CS) had the lowest M_w, which is in agreement with the literature. Moreover, potato starch (PS) and tapioca starch (TS) had a comparable M_w, which was higher than CS. Those findings are again in line with the literature (Jane et al., 1999; Vanmarcke et al., 2017). However, the exact M_w depends on the measuring technique and can vary within different botanical sources. Therefore, there does not consist an absolute value for the M_w for each specific starch source, hence different values are reported within the literature (Buléon, Colonna, et al., 1998).

WPS contains at least 99 % amylopectin, resulting in a lower R_g than PS. Similarly, TS has a lower R_g than PS, even though the M_w of TS is slightly higher. This indicates that TS should have had a higher amylopectin content than PS, as was reported in the literature (Jane et al., 1999; Millard et al., 1997; Simsek et al., 2015). The lowest R_g was reported for CS, although CS is typically high in amylose, its low M_w is dominant in the value of R_g (Buléon et al., 1998; Jane et al., 1999).

3.1.2. Influence of the botanical origin on the DS

As is visible from Table 1, the DS of S10U is always lower than that of SO. This does not follow the trend reported in the literature, in which the DS usually decreases with increasing fatty acid chain length (No Funke & Lindhauer, 2001; H. Winkler, Vorwerg, & Rihm, 2014). However, those studies involve saturated fatty acids, while our work includes unsaturated fatty acids. Our previous work shows a similar trend, in which the DS of S10U was lower than that of SO (Boetje et al., 2022). Clearly, the unsaturated bond influences the DS. Oleic acid is known to have a more compact structure than stearic acid, its saturated analog, which could explain why unsaturated fatty acids are less sterically hindered than saturated fatty acids (Bhadani et al., 2017; Fabra, Pérez-Masiá, Talens, & Chiralt, 2011). In addition, the unsaturated bond in oleic acid prevents the hydrophobic chains to stack, which accounts for its low melting point. Oleic acid has a lower melting point than 10-undecenoic acid, because 10-undecenoic acid has a double bond present at the chain end, and therefore interferes less with the chain stacking. In addition, these chains are more rigid than oleic acid, resulting in a slightly lower DS (Lide & Baysinger, 1985). No trend is observed in the DS between the different starch types. Starch with higher M_w, such as TS, has a DS similar to CS, having a low M_w. WPS had the higher DS among the different starches when esterified with oleic acid, while esterification with 10-undecenoic acid resulted in the lowest DS. Thus at least for oleic acid, esterification is not limited by steric hindrance, hence most steric hindrance is expected in highly branched starches, like WPS.

Table 1
The M_w, amylose content, the radius of gyration, and DS obtained after esterification of the studied starches.

Starch origin	Abbreviation	M_w [a] (10^6 g•mol^{-1})	Amylose content[a] (%)	R_g (nm)[a]	DS	
					S10U	SO
Potato	PS	11.9 ± 0.8	26[b]	116 ± 2.9	1.9	2.2
Waxy potato	WPS	15.5 ± 1.0	<1[c]	105 ± 2.3	1.7	2.4
Tapioca	TS	13.8 ± 1.0	27[b]	97.5 ± 2.7	1.8	2.2
Corn	CS	4.7 ± 0.2	29[b]	71.0 ± 2.3	1.7	2.1

[a] From unmodified samples.
[b] (Simsek, Ovando-Martinez, Marefati, Sj, & Rayner, 2015).
[c] (Avebe, n.d.)[a].

3.1.3. ^{1}H NMR analysis

The starch esters were analyzed by ^{1}H NMR (Fig. 1). The spectra of S10U and SO show peaks corresponding to starch (marked by the dotted square) and of the fatty acid side chain (numbered). After esterification of starch, the peaks of the AGU shifted and became broader and less pronounced, consistent with esterification (Boetje et al., 2022). All peaks in the 0–2.5 ppm range correspond to the aliphatic fatty acid part. The unsaturated bonds are expected at a higher ppm, as is the case in Fig. 1 (Boetje et al., 2022). The protons around the double bond of SO are considered similar, resulting in a single peak in the spectrum at 5.4 ppm. However, for S10U the double bond is at the fatty acid chain end, resulting in two different signals with different splitting patterns. The other starches have similar ^{1}H NMR spectra and can be found in the supplementary information in Figs. A1 and A2.

3.1.4. ATR-FTIR analysis

In addition to ^{1}H NMR spectroscopy, the products were characterized by ATR-FTIR (Fig. 2). The band intensity at 3280 cm^{-1} is reduced and shifts to 3552 cm^{-1}, indicating the substitution of the hydroxy groups of native starch. Furthermore, peaks corresponding to the aliphatic fatty acid part appeared at 2928 cm^{-1}. Similarly, carbonyl and C—O bands are present at 1740 cm^{-1} and 1149 cm^{-1}, respectively. Bands corresponding to the fatty acid double bonds are present in both spectra. For S10U, those peaks are present at 3031 and 1653 cm^{-1}, and for SO at 3008 cm^{-1}. Collectively, the results are consistent with ester formation.

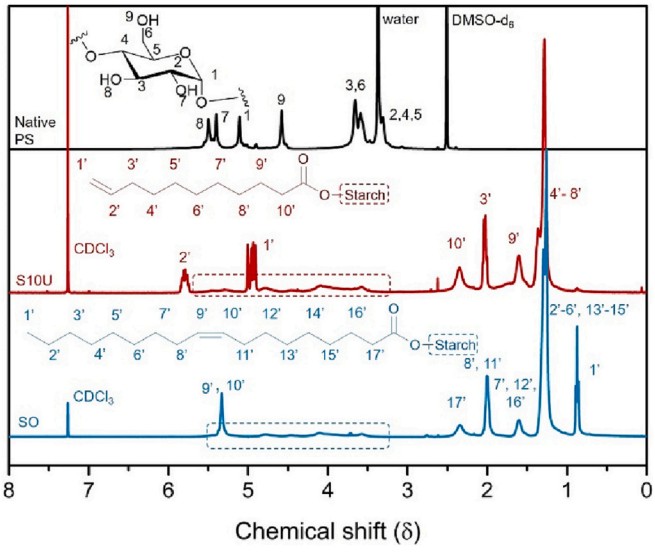

Fig. 1. ^{1}H NMR spectra of native potato starch (top - black), S10U (middle - red) and SO (bottom - blue).

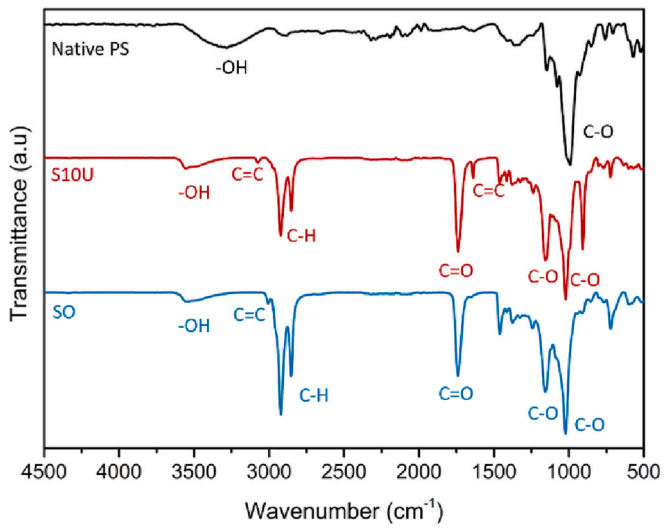

Fig. 2. ATR-FTIR spectra of native potato starch (top - black), S10U (middle - red) and SO (bottom - blue).

Similarly, for the other starches the ^{1}H NMR spectra and the FTIR spectra are similar and can be found in the supplementary information in Figs. A3 and A4.

3.2. Thermal properties

3.2.1. Thermal gravimetric analysis (TGA)

The starch esters' thermal properties were analyzed by TGA. TGA results revealed the degradation temperature (T_d) of S10U and SO (Fig. 3) and showed an increase for all starch esters compared to native starch. For S10U, the increase varied depending on the starch type from 61 to 68 °C. Fig. 3b indicates a similar behavior for SO, showing an increase in T_d of 64–71 °C after modification. Thus both starch esters showed a similar increase in the T_d which is consistent with other studies (Imre & Vilaplana, 2020; Söyler & Meier, 2017; Vanmarcke et al., 2017). Starch ester degradation starts with the cleavage of the ester bonds, followed by the starch ring that degrades. Therefore, its T_d is not influenced by the fatty acid type (Winkler et al., 2014).

Although both starch esters possessed a similar T_d, the final degradation stage is slightly different. For S10U the measurement revealed a shoulder that starts at approximately 430 °C. At this temperature, the material was already degraded for 60 wt%. From 430 °C onward, the material degrades further, and at 490 °C, the material is almost fully degraded. This shoulder between 390 and 490 °C is typical for polymers that contain 10-undecenoic acid and is caused by crosslinking of its double bond (Dutta, Chatterjee, Dhara, & Naskar, 2015; Piccini, Leak, Chuck, & Buchard, 2020). The M_w and amylopectin content did not affect the T_d, since similar values were found between the different starch sources, as supported by the literature (Vanmarcke et al., 2017).

3.2.2. Differential scanning calorimetry (DSC)

Aside from the T_d, the T_g is an important thermal property of starch ester films. Native PS without any plasticizer present has no visible T_g, but upon substitution with fatty acids, a T_g becomes visible. Above this temperature, the material can be easily processed into various shapes. Fig. 4 shows that SO films had a lower T_g than the S10U films. This is caused by the lower melting point of oleic acid, lowering the final material's T_g (Boetje et al., 2022).

In addition to the fatty acid type, the starch botanical origin is expected to influence the T_g of the starch esters. In the literature, a general trend is reported for unmodified starches with plasticizers, in which starches with a higher amylopectin content and/or M_w have a higher T_g (Zhang et al., 2014). Hence, a similar trend is expected for the modified starches reported here. Starch esters from TS possess the highest T_g, which is in line with the predictions, as TS has the highest M_w. However, CS esterified with S10U exhibited a high T_g while having both a low amylopectin content and M_w. The range of the T_g is broad and starts already just below 100 °C, which should be consistent with literature. Similarly, a lower T_g was expected for PS compared to WPS, regardless of the fatty acid used for esterification. However, for S10U the T_g is opposite to prediction. However, the DS found for S10U was lower for WPS than for PS, which is known to increase the T_g (Boetje et al., 2022). The results from SO do follow predictions. The ester from WPS does have a higher T_g than from PS, although SO from PS does have a slightly higher DS as well. It is clear that the T_g is influenced by both the DS, amylopectin content and the M_w making analysis complex.

3.3. Film morphology

3.3.1. Film appearance

Fig. 5a–d shows the film appearance of S10U and SO from PS cast at different temperatures. Films cast on a hotplate at 40 °C to 80 °C are transparent and glossy, while those cast at room temperature (20 °C) are white and opaque. The results shown in Fig. 5 are only for the films cast at 20 °C and 40 °C because the films cast at 60 °C and 80 °C showed similar results to those cast at 40 °C. Other starch sources show a similar tendency, as shown in Fig. A.5 in the Supplementary Information. This difference in appearance is a result of a difference in crystallinity, as slow solvent evaporation gives rise to a higher crystallinity, resulting in a white appearance (Koide, Ikake, Muroga, & Shimizu, 2013).

3.3.2. Polarized light microscope

Light microscopy shows that the films cast at 20 °C have a porous structure, while the films cast at 40 °C do not (Fig. 5e–h). The film cast at

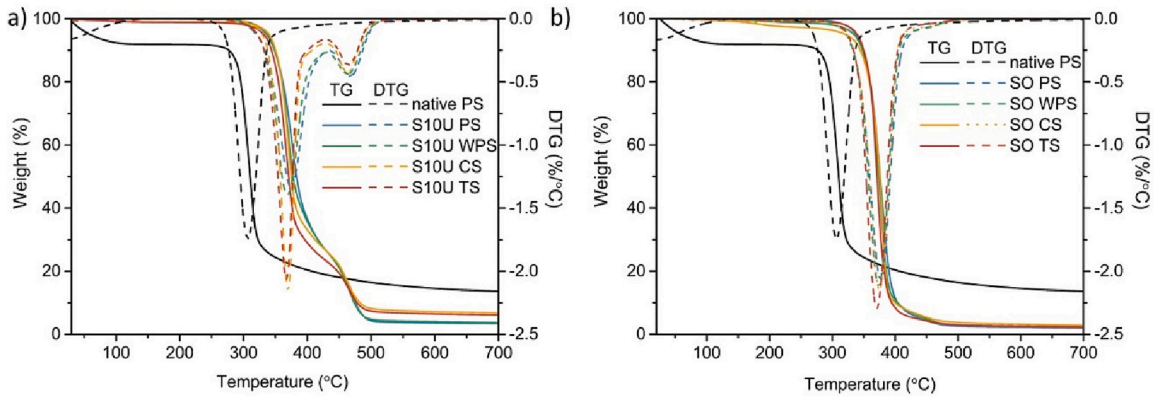

Fig. 3. Thermograms of the TG and DTG curves from different botanical origins of: a) S10U and b) SO.

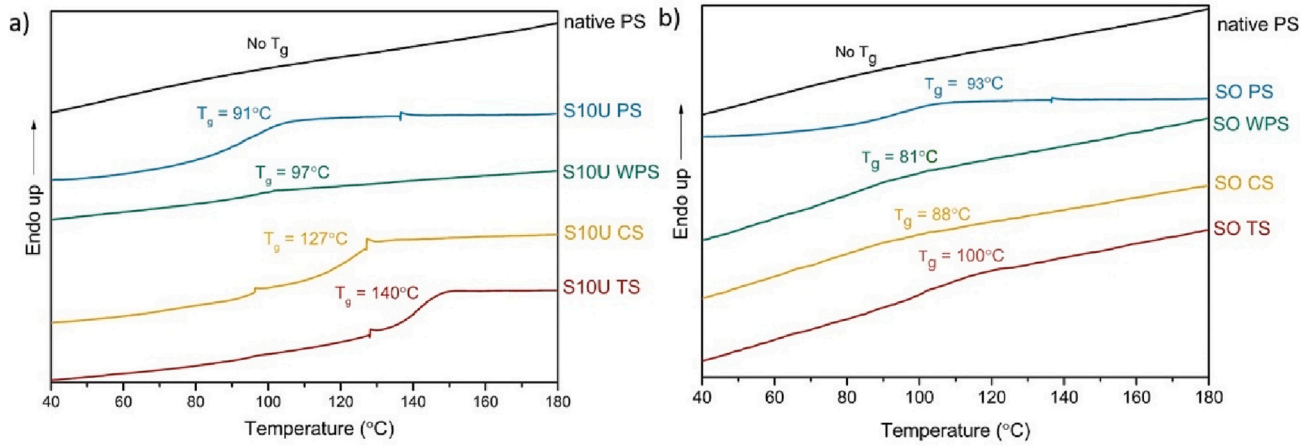

Fig. 4. DSC spectra for starches from different botanical origins of a) S10U and b) SO.

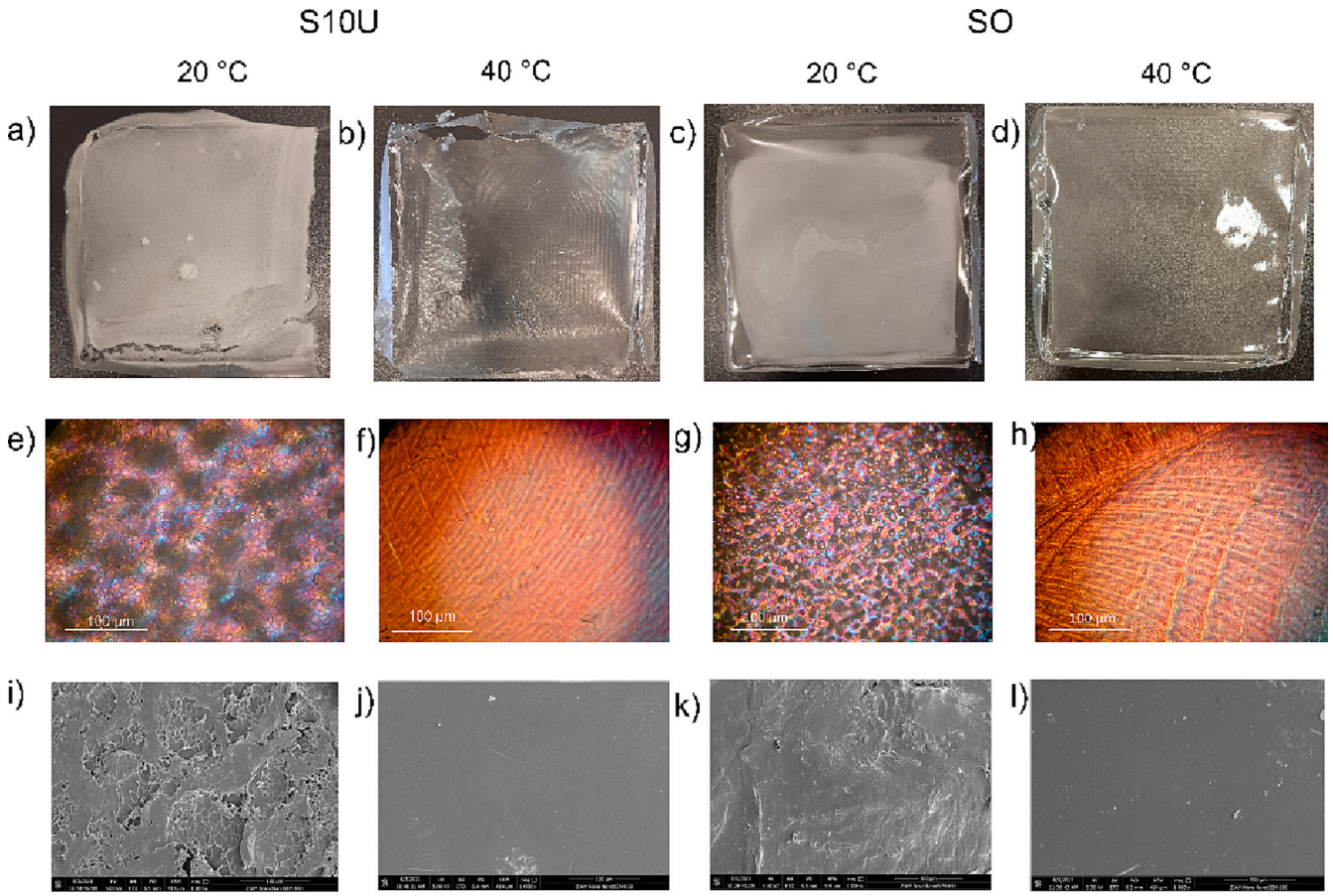

Fig. 5. Films from S10U cast at a) 20 °C and b) 40 °C, and SO at c) 20 °C and d) 40 °C. Light microscopy images under a polarized light filter of S10U cast at e) 20 °C and f) 40 °C and SO cast at g) 20 °C and h) 40 °C. *SEM* images of S10U films cast at i) 20 °C and j) 40 °C and SO cast at k) 20 °C and l) 40 °C.

40 °C shows lines that are from the structure of the Teflon mold. The rainbow color that appeared in films cast at 20 °C suggests that the material exhibits higher internal stress, which may be caused by a higher degree of order in these films (Viet, Beck-Candanedo, & Gray, 2007). This internal stress is absent for films cast at 40 °C or higher temperatures and was observed for each starch type.

3.3.3. *Scanning electron microscope (SEM)*

To better understand the film morphology, they were also analyzed by SEM. Fig. 5i–l shows the SEM images of the different films at 1000-fold magnification. The images show a porous and rough surface for S10U cast at 20 °C, whereas the film cast at 40 °C is smooth. A similar effect is observed for SO, although the film cast at 20 °C is less porous than the S10U films, but has a rougher surface than when cast at 40 °C. The porous structure might be caused by the solvent that is trapped inside the materials. The top layer already dries while there is still solvent present underneath. Upon drying, the solvent droplets break through the top layer and leave behind the porous structure. The botanical origin and the fatty acid type used did not affect the film's appearance, while the casting temperature did. By changing the casting

temperature, the transparency changed. Besides the film surface, images from the cross-sections were taken to exclude possible phase separation (Supplementary Information A.6). No phase separation or other differences in morphology were observed.

3.3.4. X-ray diffraction (XRD)

To further study the films' crystallinity, they were analyzed by XRD. The crystallinity index (CI) and the full width at half maximum (FWHM) both describe the degree of crystalline order, with a lower value indicating higher crystallinity (Crépy, Miri, Joly, Martin, & Lefebvre, 2011). First, we compared the values with native PS pregelatinized. In pregelatinized starch, the granules are already broken, and there is no crystalline order. Upon substitution with fatty acids, all starch esters show a decrease in FWHM. This indicates an increase in crystalline order for all starch esters compared to native starch. The fatty acid chains stacked, decreasing the FWHM (Boetje et al., 2022). No correlation was observed between the FHWM and the casting temperature (Fig. 6). A higher crystalline order was expected for the films cast at lower temperatures. When looking at the CI, no correlation between the casting temperature and the CI was found either. SO films did show a higher CI than S10U films, and a lower FWHM for most SO films. This was in agreement with earlier results (Boetje et al., 2022). Unfortunately, the XRD data do not support the earlier hypothesis, in which we expected that casting temperature also influenced the material crystallinity. Possibly, the internal stress observed under the polarized light microscope does not provide a high enough level of order to show in either XRD or as a T_m in DSC.

3.3.5. Mechanical properties

The films were cut into dog bone-shaped halters and those were used to determine the mechanical properties. The results for the different starches are depicted in Fig. 7a and show that films from S10U have a higher Young's modulus than SO, but are also more brittle than SO films. Other research has shown that the maximum strength decreases with increased fatty acid chain length, while the elongation at break increases, because longer side chains have a greater plasticizing effect. The starch backbone will be further apart, limiting the hydrogen bonding between the remaining hydroxyl groups (H. Winkler et al., 2014).

The botanical origin is expected to influence the films' mechanical properties. Starch ester films from TS and WPS yielded the highest mechanical strength and Young's modulus. With increasing M_w and amylopectin content, the Young's modulus increased, which agrees with the results obtained for starches containing plasticizers (Zhang et al., 2014). The native starches and starch esters from CS gave films that were brittle and broke during cutting, and therefore their mechanical properties could not be measured. Starch esters from CS were brittle because of their lower M_w (Zhang et al., 2014).

Since the casting temperature influenced the films' physical appearance, the mechanical properties at different casting temperatures were also tested. While the lowest mechanical strength was found for films cast at 20 °C, the difference was small (Fig. 7b). Generally, more crystalline samples are more brittle, meaning having a higher mechanical strength but a lower maximum elongation (Winkler et al., 2014). The results in Fig. 7b do show this behavior, but the effect is only minimal, as the difference in crystallinity is small, as shown by XRD. The tensile test revealed, as expected, that the botanical origin did influence the mechanical properties, while the casting temperature had little effect. Only for the film from S10U cast at 40 °C a clear increase in mechanical strength was observed.

Fig. 7c indicates the mechanical properties of both films after being immersed in water up to 30 days. With time, mechanical strength increased, with this effect being more evident for SO than for S10U. The increase in mechanical strength is attributed to crosslinking of the double bond over time. To confirm this hypothesis, films were immersed in chloroform, and most of the film was no longer soluble again but remained in the gel, indicating a crosslinked material. This was not observed for films that were immersed in chloroform directly after casting; instead, they fully dissolved. The fatty acid's double bond can form intra- and intermolecular crosslinks by autooxidation, which is caused by daylight (Bassas, Marqués, & Manresa, 2008; Ohtake, Onose, Kuwabara, & Kanbara, 2019). To exclude the effect of water, a similar test was performed for a sample that was left on the bench exposed to daylight but was not immersed in water. A similar result was obtained, in which the majority of the film was unable to dissolve again and remained in the gel. In addition, the sample that was exposed to daylight for one week showed a similar increase in mechanical strength (Supplementary Information A.7).

3.3.6. Antibacterial properties

Fatty acids are known to be resistant to bacteria, but to what extent they have antibacterial properties is dependent on numerous factors, such as chain length, degree of unsaturation, location of any unsaturated bonds, and their configuration (cis/trans) (McGaw, Jäger, & Van Staden, 2002; Zhao et al., 2015) The native PS, S10U, and SO were tested for antibacterial properties against *E. coli* (gram-negative) and *S. aureus* (gram-positive) bacteria. For this experiment, only PS was used since the starch type is not expected to have any influence on the antibacterial properties.

Native PS showed bacterial growth for both bacteria as expected (Table 2) (Abreu et al., 2015). For S10U, the number of *E. coli* and *S. aureus* bacteria measured, were comparable. The SO film contained a similar amount of *S. aureus*, whereas no *E. coli* was detected, indicating

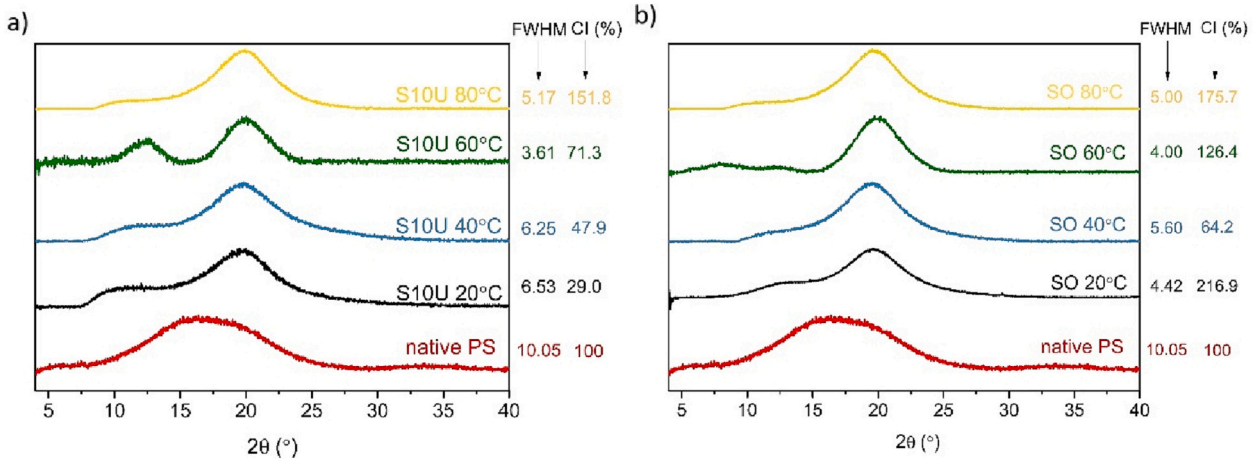

Fig. 6. XRD patterns of a) S10U and b) SO with their FWHM when cast at different temperatures.

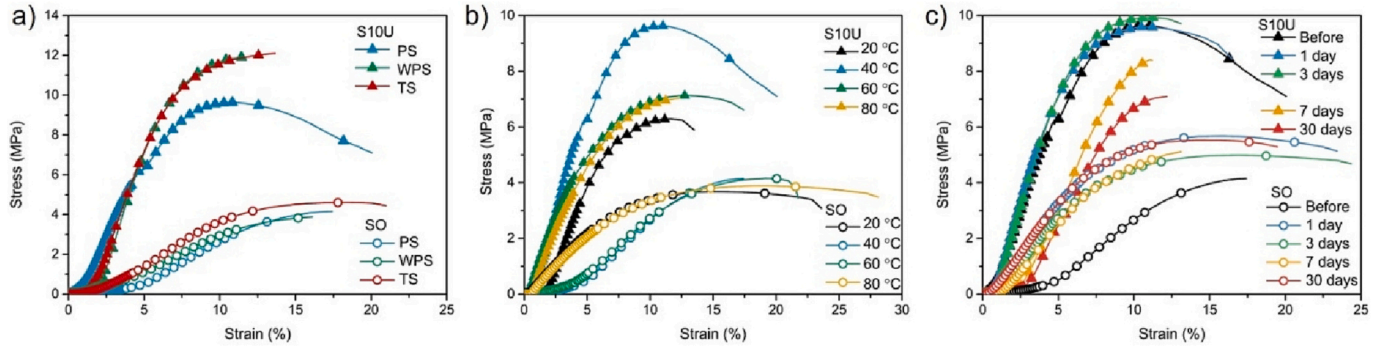

Fig. 7. The mechanical properties of S10U (▲) and SO(○) films a) from starches with different botanical origins, b) from PS cast at different temperatures, and c) after being immersed in water at different time intervals.

Table 2
Results of the petrifilm test. The red dot indicates the number of bacteria present on each film after incubation.

	Native PS	S10U	SO
E. coli	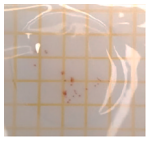	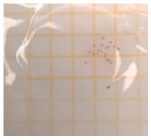	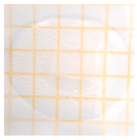
S. aureus	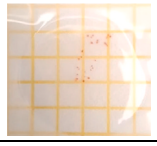	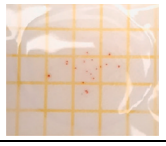	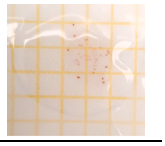

that oleic acid introduced an antibacterial effect on *E. coli* growth but not on *S. aureus*. Oleic acid is known to have slight antibacterial effects on gram-positive bacteria such as *S. aureus* (Sheu, Salomon, Simmons, Sreevalsan, & Freese, 1975), which is in line with the results of this study. Similar results were reported for sucrose oleates, in which esterification has a positive effect on gram-positive bacteria inhibition. Although the sucrose oleate esters were still found to be incapable of inhibiting the *S. aureus* growth, which is consistent with the current findings (Conley & Kabara, 1973; Dilika et al., 2000).

Although no literature was found on the antibacterial properties of sugar esters from 10-undecenoic acid, a polyester with a 10-undecenoic acid side chain showed some antibacterial properties against *S. aureus* and little toward *E. coli* (Totaro et al., 2014). These findings do not support the results in our study since no antibacterial effect was observed for either *E. coli* or *S. aureus*. At this point, it is impossible to determine what causes the absence of antibacterial properties in the S10U films since its effectiveness depends on many factors and might even be different between different bacteria strains (Toshkova-Yotova et al., 2022). However, the results do show that depending on the fatty acid type, such as oleic acid, starch esters can possess antibacterial properties.

This study compared the influence of the fatty acid type, the botanical origin, and the casting temperature on the film properties. Table 3, summarizes whether the variables do have an influence on each specific film property.

4. Conclusion

A series of different starches with varying amylopectin contents and M_w values were successfully esterified with 10-undecenoic acid and oleic acid. A maximum DS of 1.9 was obtained for S10U, while for SO, the maximum was 2.4. Although the DS was similar for each starch type, the maximum DS was obtained for S10U and SO for PS and WPS, respectively. A T_g is visible after esterification for all starch esters and a higher T_g was observed for S10U than for SO, which is ascribed to the higher melting point of 10-undecenoic acid. The mechanical properties were affected by starch's botanical origin. Higher amylopectin content and M_w resulted in higher mechanical strength. CS-based films were too brittle to be tested, due to its low M_w. Films from S10U have higher Young's moduli than SO, because SO has a longer fatty acid chain with a greater plasticizing effect. The highest mechanical strength was observed for S10U (12.1 MPa) and SO (4.6 MPa), both for TS. Solvent casting resulted in a white and semitransparent film when cast at 20 °C, while when cast at elevated temperatures, transparent films were obtained. SEM revealed a porous structure for the films cast at 20 °C, while the films cast at a higher temperature were smooth. Polarized light microscopy showed a similar structure. Moreover, polarized light microscopy also revealed that the films had a white color which is caused by internal stress and is absent in the films cast at a higher temperature. However, XRD showed that this stress did not lead to the formation of crystalline domains. SO films are antibacterial against *E. coli* in contrast to PS and S10U and no antibacterial effect was observed for any of the films against *S. aureus*. These results provide more insight into the effect of the starch type on the thermal and mechanical properties and how the casting temperature can influence the appearance and the fatty acids affect the antibacterial properties.

CRediT authorship contribution statement

Laura Boetje: Conceptualization, Methodology, Validation, Formal analysis, Investigation, Writing – Original draft and Visualization. **Xiaohong Lan:** Conceptualization, Writing- Reviewing and Editing. **Jur van Dijken:** Formal Analysis and Writing- Reviewing & Editing **Albert Woortman:** Formal Analysis and Writing- Reviewing and Editing. **Thijs**

Table 3
Different parameters were used to study the effect on the film properties.

	DS	Thermal properties		Physical appearance	Mechanical properties	Antibacterial properties
		T_g	T_d			
Fatty acid type	+	+			+	+
Botanic origin	+				+	
Casting temperature				+	±	

Popken: Methodology and Formal Analysis, **Michael Polhuis:** Writing-Reviewing and Editing, Supervision. **Katja Loos:** Writing- Reviewing and Editing, Supervision, Project administration, Funding acquisition.

Declaration of competing interest

The authors declare that they have no known competing financial interests or personal relationships that could have appeared to influence the work reported in this paper.

Data availability

Data will be made available on request.

Acknowledgments

This research was performed in the public private partnership CarboBased, coordinated by the Carbohydrate Competence Center (CCC, www.cccresearch.nl) and cofinanced by the "Samenwerkingsverband Noord-Nederland (SNN), Ruimtelijk Economisch Programma". We thank prof. dr. Henny van der Mei and Marja Slomp for their help with the antibacterial tests.

Appendix A. Supplementary data

Supplementary data to this article can be found online at https://doi.org/10.1016/j.carbpol.2023.121043.

References

Abreu, A. S., Oliveira, M., De Sá, A., Rodrigues, R. M., Cerqueira, M. A., Vicente, A. A., & Machado, A. V. (2015). Antimicrobial nanostructured starch based films for packaging. *Carbohydrate Polymers, 129*, 127–134.

Ahmadi-Abhari, S., Woortman, A. J. J., Hamer, R. J., & Loos, K. (2015). Rheological properties of wheat starch influenced by amylose-lysophosphatidylcholine complexation at different gelation phases. *Carbohydrate Polymers, 122*, 197–201.

Avebe. (n.d.). ElianeTM Commercial Leaflet.

Bassas, M., Marqués, A. M., & Manresa, A. (2008). Study of the crosslinking reaction (natural and UV induced) in polyunsaturated PHA from linseed oil. *Biochemical Engineering Journal, 40*, 275–283.

Bhadani, A., Iwabata, K., Sakai, K., Koura, S., Sakai, H., & Abe, M. (2017). Sustainable oleic and stearic acid based biodegradable surfactants. *RSC Advances, 7*, 10433–10442.

Blohm, S., & Heinze, T. (2019). Synthesis and properties of thermoplastic starch laurates. *Carbohydrate Research, 486*, Article 107833.

Boetje, L., Lan, X., Silvianti, F., van Dijken, J., Polhuis, M., & Loos, K. (2022). A more efficient synthesis and properties of saturated and unsaturated starch esters. *Carbohydrate Polymers, 292*, Article 119649.

Buléon, A., Colonna, P., Planchot, V., & Ball, S. (1998). Starch granules: Structure and biosynthesis. *International Journal of Biological Macromolecules, 23*, 85–112.

Buléon, A., Gallant, D. J., Bouchet, B., Mouille, G., D'Hulst, C., Kossmann, J., & Ball, S. (1998). Starches from A to C (Chlamydomonas reinhardtii as a model microbial system to investigate the biosynthesis of the plant amylopectin crystal). *Starch - Stärke, 46*, 56.

Chandrasekaran, M., Senthilkumar, A., & Venkatesalu, V. (2011). Antibacterial and antifungal efficacy of fatty acid methyl esters from the leaves of Sesuvium portulacastrum L. *European Review for Medical and Pharmacological Sciences, 15*(7), 775–780.

Ciardelli, F., & Penczek, S. (2004). *Modification and blending of synthetic and natural macromolecules*. Dordrecht: Kluwer Academic Publishers.

Conley, A. J., & Kabara, J. J. (1973). Antimicrobial action of esters of polyhydric alcohols. *Pharmacologist, 15*, 545.

Costas, G. B. (1998). Structures and phase transitions of starch polymers. In *Polysaccharide association structures in food*. New York.

Crépy, L., Miri, V., Joly, N., Martin, P., & Lefebvre, J. (2011). Effect of side chain length on structure and thermomechanical properties of fully substituted cellulose fatty esters. *83*, 1812–1820.

Dilika, F., Bremner, P. D., & Meyer, J. J. M. (2000). Antibacterial activity of linoleic and oleic acids isolated from Helichrysum pedunculatum: A plant used during circumcision rites. *Fitoterapia, 71*, 450–452.

Dutta, J., Chatterjee, T., Dhara, G., & Naskar, K. (2015). Exploring the influence of electron beam irradiation on the morphology, physico-mechanical, thermal behaviour and performance properties of EVA and TPU blends. *RSC Advances, 5*, 41563–41575.

Fabra, M. J., Pérez-Masiá, R., Talens, P., & Chiralt, A. (2011). Influence of the homogenization conditions and lipid self-association on properties of sodium caseinate based films containing oleic and stearic acids. *Food Hydrocolloids, 25*, 1112–1121.

Fang, J. M., Fowler, P. A., Tomkinson, J., & Hill, C. A. S. (2002). The preparation and characterization of a series of chemically modified potato starches. *Carbohydrate Polymers, 47*, 245–252.

Fredriksson, H., Silverio, J., Andersson, R., Eliasson, A. C., & Åman, P. (1998). The influence of amylose and amylopectin characteristics on gelatinization and retrogradation properties of different starches. *Carbohydrate Polymers, 35*, 119–134.

French, D. (1972). Fine structure of starch and its relationship to the Organization of Starch Granules. *Journal of the Japanese Society of Starch Science, 19*, 8–25.

Harris, L. J. (1997). Microbial pathogens associated with produce. *Perishables Handling Quarterly, 91*, 2–3.

Heinze, T., Libert, T., & Koschella, A. (2006). *Esterification of polysaccharides*. Berlin: Springer.

Huang, T., Qian, Y., Wei, J., & Zhou, C. (2019). Polymeric antimicrobial food packaging and its applications. *Polymers, 11*, 560.

Hussain, M. A., Liebert, T., Heinze, T., & Jena, D. (2004). *Acylation of cellulose with N, N 0 -carbonyldiimidazole- activated acids in the novel solvent dimethyl sulfoxide / tetrabutylammonium fluoride. 101* pp. 916–920).

Imre, B., & Vilaplana, F. (2020). Organocatalytic esterification of corn starches towards enhanced thermal stability and moisture resistance. *Green Chemistry, 22*, 5017–5031.

Jane, J., Chen, Y. Y., Lee, L. F., McPherson, A. E., Wong, K. S., Radosavljevic, M., & Kasemsuwan, T. (1999). Effects of amylopectin branch chain length and amylose content on the gelatinization and pasting properties of starch. *Cereal Chemistry, 76*, 629–637.

Keskin, D., Tromp, L., Mergel, O., Zu, G., Warszawik, E., Van Der Mei, H. C., & Van Rijn, P. (2020). Highly efficient antimicrobial and antifouling surface coatings with triclosan-loaded nanogels. *ACS Applied Materials and Interfaces, 12*, 57721–57731.

Koide, Y., Ikake, H., Muroga, Y., & Shimizu, S. (2013). Effect of the cast-solvent on the morphology of cast films formed with a mixture of stereoisomeric poly(lactic acids). *Polymer Journal, 45*, 645–650.

Konieczny, J., & Loos, K. (2018). Facile esterification of degraded and non-degraded starch. *Macromolecular Chemistry and Physics, 219*, 1–4.

Lide, D. R., & Baysinger, G. (1985). In W. M. Haynes, D. R. Lide, & T. J. Bruno (Eds.), *Handbook of chemistry and physics*. Baco Raton: Taylor & Francis Group.

Malhotra, B., Keshwani, A., & Kharkwal, H. (2015). Antimicrobial food packaging: Potential and pitfalls. *Frontiers in Microbiology, 6*, 1–9.

McGaw, L. J., Jäger, A. K., & Van Staden, J. (2002). Antibacterial effects of fatty acids and related compounds from plants. *South African Journal of Botany, 68*, 417–423.

Millard, M. M., Dintzis, F. R., Willett, J. L., & Klavons, J. A. (1997). Light-scattering molecular weights and intrinsic viscosities of processed waxy maize.Pdf. *Cereal Chemistry, 74*, 687–691.

Motelica, L., Ficai, D., Ficai, A., Oprea, O. C., Kaya, D. A., & Andronescu, E. (2020). Biodegradable antimicrobial food packaging: Trends and perspectives. *Foods, 9*, 1–36.

Mua, J. P., & Jackson, D. S. (1997). Fine structure of corn amylose and amylopectin fractions with various molecular weights. *Journal of Agricultural and Food Chemistry, 45*, 3840–3847.

Niranjana Prabhu, T., & Prashantha, K. (2018). A review on present status and future challenges of starch based polymer films and their composites in food packaging applications. *Polymer Composites, 39*, 2499–2522.

No Funke, U., & Lindhauer, M. G. (2001). Effect of reaction conditions and alkyl chain lengths on the properties of hydroxyalkyl starch ethers. *Starch - Stärke, 53*, 547–554.

Ohtake, K., Onose, Y., Kuwabara, J., & Kanbara, T. (2019). Postfunctionalization of reactive polyolefins derived from fatty acids. *Reactive and Functional Polymers, 139*, 17–24.

Perinelli, D. R., Lucarini, S., Fagioli, L., Campana, R., Vllasaliu, D., Duranti, A., & Casettari, L. (2018). Lactose oleate as new biocompatible surfactant for pharmaceutical applications. *European Journal of Pharmaceutics and Biopharmaceutics, 124*, 55–62.

Piccini, M., Leak, D. J., Chuck, C. J., & Buchard, A. (2020). Polymers from sugars and unsaturated fatty acids: ADMET polymerisation of monomers derived from d-xylose, d-mannose and castor oil. *Polymer Chemistry, 11*, 2681–2691.

Sheu, C. W., Salomon, D., Simmons, J. L., Sreevalsan, T., & Freese, E. (1975). Inhibitory effects of lipophilic acids and related compounds on bacteria and mammalian cells. *Antimicrob.Agents Chemother., 7*, 349–363.

Simsek, S., Ovando-Martinez, M., Marefati, A., Sj, M., & Rayner, M. (2015). Chemical composition, digestibility and emulsification properties of octenyl succinic esters of various starches. *Food Research International, 75*, 41–49.

Söyler, Z., & Meier, M. A. R. (2017). Sustainable functionalization of cellulose and starch with diallyl carbonate in ionic liquids. *Green Chemistry, 19*, 3899–3907.

Sung, S. Y., Sin, L. T., Tee, T. T., Bee, S. T., Rahmat, A. R., Rahman, W. A. W. A., & Vikhraman, M. (2013). Antimicrobial agents for food packaging applications. *Trends in Food Science and Technology, 33*, 110–123.

Tharanathan, R. N. (2003). Biodegradable films and composite coatings: Past, present and future. *Trends in Food Science and Technology, 14*, 71–78.

Toshkova-Yotova, T., Georgieva, A., Iliev, I., Alexandrov, S., Ivanova, A., Pilarski, P., & Toshkova, R. (2022). Antitumor and antimicrobial activity of fatty acids from green microalga Coelastrella sp. BGV. *South African Journal of Botany, 000*, 1–9.

Totaro, G., Cruciani, L., Vannini, M., Mazzola, G., Di Gioia, D., Celli, A., & Sisti, L. (2014). Synthesis of castor oil-derived polyesters with antimicrobial activity. *European Polymer Journal, 56*(1), 174–184.

Van Soest, J. J. G., Hulleman, S. H. D., De Wit, D., & Vliegenthart, J. F. G. (1996). Crystallinity in starch bioplastics. *Industrial Crops and Products, 5*, 11–22.

Van Soest, J. J. G., & Vliegenthart, J. F. G. (1997). Crystallinity in starch plastics: Consequences for material properties. *Trends in Biotechnology, 15*, 208–213.

Vanmarcke, A., Leroy, L., Stoclet, G., Duchatel-Crépy, L., Lefebvre, J. M., Joly, N., & Gaucher, V. (2017). Influence of fatty chain length and starch composition on structure and properties of fully substituted fatty acid starch esters. *Carbohydrate Polymers, 164*, 249–257.

Viet, D., Beck-Candanedo, S., & Gray, D. G. (2007). Dispersion of cellulose nanocrystals in polar organic solvents. *Cellulose, 14*, 109–113.

Winkler, H., Vorwerg, W., & Rihm, R. (2014). Thermal and mechanical properties of fatty acid starch esters. *Carbohydrate Polymers, 102*, 941–949.

Winkler, H., Vorwerg, W., & Wetzel, H. (2013). Synthesis and properties of fatty acid starch esters. *Carbohydrate Polymers, 98*, 208–216.

Zhang, Y., Rempel, C., & Liu, Q. (2014). Thermoplastic starch processing and characteristics-a review. *Critical Reviews in Food Science and Nutrition, 54*, 1353–1370.

Zhang, Y., Liu, X., Wang, Y., Jiang, P., & Quek, S. Y. (2016). Antibacterial activity and mechanism of cinnamon essential oil against Escherichia coli and Staphylococcus aureus. *Food Control, 59*, 282–289.

Zhao, L., Zhang, H., Hao, T., & Li, S. (2015). In vitro antibacterial activities and mechanism of sugar fatty acid esters against five food-related bacteria. *Food Chemistry, 187*, 370–377.

Zhu, J., Zhang, S., Zhang, B., Qiao, D., Pu, H., & Liu, S. (2017). Structural features and thermal property of propionylated starches with different amylose / amylopectin ratio. *International Journal of Biological Macromolecules, 97*, 123–130.